A bound-constrained solver for phase-field modelling of diffuse fracture

Matheus M. Fortes[1], Hugo M. Leão[1], Rafael G. Bayão[2], Lapo Gori[1], Roque S. Pitangueira [1]

[1]*Structural Engineering Graduate Course at the Federal University of Minas Gerais*
Av. Antônio Carlos, 6627, Pampulha, 31270-901, Minas Gerais, Brazil
matheuseng97@gmail.com,hugomleao@yahoo.com.br,lapo@dees.ufmg.br,roque@dees.ufmg.br
[2]*Mechanical Engineering Undergraduate Course at the Federal University of Minas Gerais*
Av. Antônio Carlos, 6627, Pampulha, 31270-901, Minas Gerais, Brazil
rgbayao@gmail.com

Abstract. In a structural analysis it is important to know the propagation of cracks to prevent a possible failure of the material or the structure. One way to model a crack is by the phase-field strategy. Within this approach, the problem is described by the displacements field and by an additional variable, the phase-field, that measures the degradation of the material, like a damage variable. Using this variable, a crack is represented in a smooth and diffuse way. In the current version of the INSANE (INteractive Structural ANalysis Environment system), an open-source software developed at the Department of Structural Engineering (DEES) of the Federal University of Minas Gerais (UFMG), some phase-field models have been implemented. However such models have certain limitations, due to how the crack irreversibility condition is handled. The present work proposes to remove these limitations with the implementation of a bound-constrained solver that, as pointed out in the literature, constitutes a more general approach to deal with the irreversibility condition. In the implementation, the library PETSc (Portable, Extensible Toolkit for Scientific Computation) is used. Numerical simulations are presented to illustrate the characteristics of the implementation.

Keywords: diffusive crack; phase-field; bound-constrained solver

1 Introduction

One of the several important issues in structural engineering is fracture mechanics, and a scope of research is the path the crack will take on. Cracking can be described in two ways, which are the discrete and the continuous form. In the discrete approach, cracks are modelled as displacement discontinuities in the domain, while in the continuous approach the displacements are continuous, but the stiffness is gradually reduced to model the material degradation process. One of the ways to treat the degradation process, that has been increasingly used, is the phase-field aprroach.

The phase-field is a scalar variable that goes from 1 for the fully cracked state of the material to 0 for the undameged state. In addition to the phase-field parameter, another parameter is the length scale parameter, that controls the width of the region where the discrete crack is smoothed on. Small values of this length tends to reproduce the Griffith's theory.

The phase-field has already been widely discussed by several authors. A complete review on the theme of phase-field, which addresses several references on the subject, can be found in Wu et al. [1]. An important question on phase-field models is how the issue of irreversibility of the crack is handled. Depending on the used strategy, may be limitations on the model. In order to overcome such a limitation in INSANE, this work focused on the implementation of a bounded-constrained solver using the library PETSc (Balay et al. [2]).

2 Phase-Field Theory

The starting point for the phase-field theory is a domain Ω with boundary $\partial\Omega$ and a crack Γ. The boundary region where prescribed displacements are applied on is indicated by $\partial\Omega_u$, while indicates the part of the boundary

where prescribed tractions are applied on $\partial\Omega_t$.

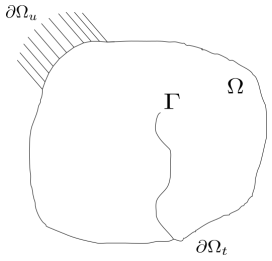

Figure 1. A solid body with a crack.

Within the phase-field approach, the total energy functional E_t is given by:

$$E_t(\vec{u},\phi) = \int_\Omega \psi(\underline{\varepsilon}(\bar{u}),\phi)\,\mathrm{d}\mathcal{V} + \int_\Omega G_c\gamma(\phi,\nabla\phi)\,\mathrm{d}\mathcal{A} - \int_\Omega \bar{b}\cdot u\,\mathrm{d}\mathcal{V} - \int_{\partial\Omega} \bar{t}\cdot u\,\mathrm{d}\mathcal{A} \tag{1}$$

where $\bar{u}$ is the displacements field, ϕ is the phase-field, ψ is the strain energy density (see more in section 2.2), G_c is a material property that represents the critical energy release rate, γ is the crack surface density function (see more in section 2.1), $\bar{b}$ is the body forces and $\bar{t}$ is the surface forces.

2.1 Crack Surface Desinty Function

The crack surface density function γ in eq. (1) describes how the sharp crack topology is smoothed over the domain. Wu [3] proposed a general equation for the surface density function of the crack:

$$\gamma(\phi,\nabla\phi) = \frac{1}{C_0}\left[\frac{1}{l_0}\alpha(\phi) + l_0|\nabla\phi|^2\right] \tag{2}$$

where the *crack geometry function* $\alpha(\phi)$ and the parameter $C_0 = 4\int_0^1 \alpha^{1/2}(\phi)d\phi$ have been introduced. The function $\alpha(\phi)$ determines how the phase-field will be distributed and it has to satisfy the following properties: $\alpha(0) = 0$ and $\alpha(1) = 1$. Wu [3] proposed the following quadratic equation for α:

$$\alpha(\phi) = \xi\phi + (1-\xi)\phi^2 \in [0,1] \quad \forall\phi \in [0,1] \tag{3}$$

where $\xi \in [0,2]$, otherwise $\alpha(\phi) \in [0,1]$ cannot be guaranted.

2.2 Energy Degradation Function

The strain energy function, in eq. (1), describes a smooth transition between the fully broken and fully unbroken states of the material. The *initial strain energy density function* $\psi_0(\bar{\varepsilon})$ and the degradation function $g(\phi) : [0,1] \longrightarrow [1,0]$ are used to describe the strain energy function.

An anisotropic formulation was proposed to prevent crack formation in compressed regions, based on the following additive decomposition of the elastic strain energy:

$$\psi_0(\underline{\varepsilon}) = \psi_0^+(\underline{\varepsilon}) + \psi_0^-(\underline{\varepsilon}) \tag{4}$$

where $\psi_0^+(\underline{\varepsilon})$ is the part that comes from tensile (active strain energy density) and $\psi_0^-(\underline{\varepsilon})$ is the part of compression (inactive strain energy density). The degradation is then assumed to affect just the tensile part:

$$\psi(\underline{\varepsilon}) = g(\phi)\psi_0^+(\underline{\varepsilon}) + \psi_0^-(\underline{\varepsilon}) \tag{5}$$

The energy degradation function, $g(\phi)$, makes the connection between the crack phase-field and the mechanical fields. There are many energy degradation function, $g(\phi)$, already proposed in the literature. In this work the focus is the $g(\phi)$ function proposed by Wu [3]:

$$g(\phi) = \frac{(1-\phi)^p}{(1-\phi)^p + Q(\phi)} \tag{6}$$

where the exponent $p > 0$ and continuous function $Q(\phi) > 0$ is given by:

$$Q(\phi) = c_1\phi + c_1c_2\phi^2 + c_1c_2c_3\phi^3 + \cdots \tag{7}$$

where c_1, c_2 and c_3 are given by:

$$c_1 = \frac{2E_0G_c}{f_t^2}\frac{\xi}{C_0l_0} = \frac{2\xi}{C_0}\frac{l_{ch}}{l_0} \tag{8}$$

$$c_2 = \frac{1}{\xi}[(-\frac{4\pi\xi^2}{C_0}\frac{G_c}{f_t^2}k_0) - (p+1)] \tag{9}$$

$$c_3 = \begin{cases} 0 \quad p > 2 \\ \frac{1}{c_2}[\frac{1}{\xi}(\frac{C_0w_cf_t}{2\pi G_c})^2 - (1+c_2)] \quad p = 2 \end{cases} \tag{10}$$

where E_0 is the Young´s modulus, f_t is the failure strength and $l_{ch} = E_0G_c/f_t^2$ is the characteristic length, for Griffith´s or Irwin´s theories. w_c is the ultimate apparent displacement jump (ultimate crack opening) and k_0 is the initial slope for the softening curves, which represent the relationship between the stress (σ) and the apparent displacement jump (w) across the localisation band. More details on the parameters w_c and k_0, and on the different ways they can be obtained, can be found in Wu [3].

2.3 Irreversibility Condition

To find the displacement and the phase-field $(\bar{u}, \phi)$ it's necessary to minimise the total energy functional of eq. (1), imposing also the irreversibility ($\phi \geq 0$) and bounding ($\phi \in [0, 1]$). There are different ways to impose such conditions. For example, Bourdin et al. [4] proposed to the irreversibility condition when the crack phase-field is close to one: $\phi(x, t > t_0) = 1$ if $\phi(x, t_0) \approx 1$. Miehe et al. [5] has considered the *effective crack driving force* as a historical variable ($\mathcal{H}$) that represents the maximum tensile energy that the material had experimented. This strategy has been widely used in the literature, and is the one adopted by Leão [6], but it can only be used for $\alpha(\phi) = \phi^2$, which makes $\xi = 0$ and cannot use the eq. (6) for $g(\phi)$.

Others authors focused directly on a constrained minimisation of the energy function, using some type of bound-constrained solver. Farell and Maurini [7] and Wu [8] used the PETSc library to solve the constrained minimisation problem with the reduced space active set method, based in the work Benson and Munson [9].This method will be discussed in section 3, because it was chosen to be adopted in this work, in order to to circumvent the condition of irreversibility.

2.4 Equations of Phase-Field Models in Weak Form

The governing equations of a phase-field model are:

$$\begin{cases} \int_\Omega \underline{\sigma} : \delta\underline{\varepsilon}\, \mathrm{d}\mathcal{V} = \delta P_{ext} \\ \int_\mathcal{B} \left[g'(\phi)\bar{Y}\delta\phi + G_c\dfrac{1}{l_0}\alpha'(\phi)\delta\phi + 2l_0\nabla\phi\cdot\nabla\delta\phi \right] \mathrm{d}\mathcal{V} \geq 0 \end{cases} \tag{11}$$

where $\bar{Y} = \dfrac{\partial \psi}{\partial g}$ is the *effective crack driving force*. More details on the development of the equation can be found in Wu et al. [1].

3 Bound-Constrained Solver

To deal with the boundedness and irreversibility conditions, it's convenient to regard the governing equation from residual phase-field form as an optimization problem bounded by the following condition:

$$0 \leq a_{I,n} \leq a_{I,n+1} \leq 1 \tag{12}$$

‘

where $\bar{a}$ is phase-field nodal, n is the current step, $n+1$ is the next step and I is the index for each node. The residual phase-field form is obtained through the development of discretization by finite element method of phase-field in weak form (section 2.4), more details in Wu et al. [1]. The phase-field nodal is described by the relation $\phi(\bar{x}) = [\mathbf{N}]^{\phi}\,\bar{a}$, where $[\mathbf{N}]^{\phi}$ is the shape function for phase-field variable.

According to Farell and Maurini [7], under the above condition the residual phase-field equation constitutes a mixed complementarity problem(MCP), which is a problem formulation in mathematical programming. That can be written as:

$$\begin{cases} a_{I,n} < a_{I,n+1} < 1 \quad r_I^{\phi} = 0 \\ a_{I,n} = a_{I,n+1} \quad r_I^{\phi} \leq 0 \\ a_{I,n+1} = 1 \quad r_I^{\phi} \geq 0 \end{cases} \tag{13}$$

where r_I^{ϕ} is the residual phase-field form. The Equation 13 says that the solution of residual phase-field equation needs to be for each node, precisely, one of the conditions shown. For solve this like Wu et al. [1] and Farell and Maurini [7], this work intends to use a reduced-space active set Newton method, included in the the open-source toolkit PETSc (Balay et al. [2]). This solver is based on work of Benson and Munson [9], and its main idea is placed in the Fig. 2.

Data: a^0, $k = 0$
Result: A solution of (r^{ϕ})
Given a^0, the initial guess
while $||\bar{r}^{\phi}(a^k)|| > TOL$ **do**
  Compute active($\mathscr{A}$) and inactive($\mathscr{I}$) sets:
  $\mathscr{A}(a) = a_{I,n+1} = a_{I,n}$ `and` $r^{\phi} < 0$ *or* $a_{I,n+1} = 1$ `and` $r^{\phi} > 0$
  $\mathscr{I}(a) = 1 > a_{I,n+1} > a_{I,n}$ `and` $r^{\phi} = 0$
  Set $\bar{dir}_{\mathscr{A}} = 0$, where $\bar{dir}$ is the direction of the line search
  Solve the reduce Newton step for $\bar{dir}_{\mathscr{I}}$:
  $[\nabla \bar{r}^{\phi}(a^k)]_{\mathscr{I}^k,\mathscr{I}^k} \bar{dir}_{\mathscr{I}^k} = -\bar{r}^{\phi}_{\mathscr{I}^k}(a^k)$
  Choose the step length μ such that $||r^{\phi}||^2$ is minimized, via line search on $\bar{a}^{k+1} = \bar{a}^k + \mu\, dir$; if this search direction fails, use the steepest descent direction instead.
end

Figure 2. Reduced-space active-set method adapted from Benson and Munson [9]

In the algorithm the active set is the subdomain with the restrictions applied and no equation is solved, while in the inactive set the equations are solved, in such way that the restrictions are satisfied. So the idea of the algorithm is to reduce the number of equations to be solved at each step, as it updates the inactive set.

The bound-constrained solver was implemented by PETSc and another bound-constrained solver that doesn't make use of the PETSc library. In order to use PETSc, will be do a binding to INSANE, because INSANE is written in language Java and PETSc written in language C. To do this, it will be a binding with Java Native Interface (JNI) based on the work of Azevedo [10].

4 Numerical Examples

4.1 Tension Test

The first example used to evaluate the bound-constrained solver implementation is a tension test. Furthermore, we compare the processing time between the bound-constrained solver by PETSc and another bound-constrained solver that doesn't make use of the PETSc library.

The problem is illustrated in Fig. 3 with the units in millimeters. The problem is modelled as a plane-strain state and the values used for the numerical model were: $E_0 = 210$ N/mm^2, Poisson´s ratio $\nu = 0.18$, $G_c = 0.09$ N/mm and $l_0 = 0.0015$ mm. Failure strength f_t was not considered, because for this problem used the constitutive model presented by Miehe et al. [5]. For crack geometry function was used $\alpha = \phi^2$, and for energy degradation function was used $g = (1 - \phi)^2$ (Bourdin et al. [4]). Displacement strategy control is was used considering increments of $1 \cdot 10^{-4}$ mm in all nodes of the top edge. The local tolerance used was of $1 \cdot 10^{-4}$ and the global tolerance was of $1 \cdot 10^{-3}$, where local tolerance refers to the separate convergence of displacement and phase-field variables, while the global tolerance checks if the displacement convergence, after the phase-field convergence, was not unbalanced, it would be a local displacement tolerance after the phase-field convergence. The results of the load-displacements and contour plots of phase-field for tension test are presented in Fig. 4.

The result is validated by the historical solver presented by Leão [6], comparing the load-displacement curves. Comparing the times between the PETSc solver and solver that doesn't make use of the PETSc library, the PETSc solver took 2 hours 4 minutes, while the other took 2 hours 51 minutes. Showing that as expected, an optimized library was faster.

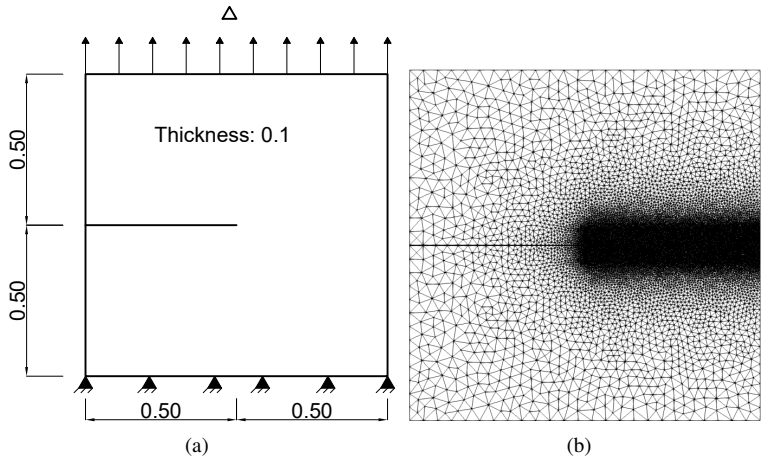

Figure 3. Tension test. (a) Problem setting.(b) T3 mesh ($h = 0.05$ mm in the unrefined region and $h = 0.001$ mm in the refined region).

4.2 Single-edge notched beam test

This second example is the single edge-notched beam under proportional loading reported by M. Arrea [11]. The objective is to compare the result of the phase-field curve obtained with the experimental results presented in M. Arrea [11].

The problem data are presented in Fig. 5 with the units in millimeters and the notch is 14 mm wide. The problem is defined in plain stress and the values used for the numerical model were: $E_0 = 24800$ N/mm^2, $\nu = 0.18$ and $l_0 = 2.5$ mm. For this problem, the constitutive model used was presented by Wu [8]. For crack geometry function was used the eq. (3) with $\xi = 2$, and for energy degradation function was used eq. (6) with Cornelissens's law for concrete (more details in Wu [3]). Displacement control strategy was used considering increments of $1 \cdot 10^{-3}$ mm in the right node of the crack. The local tolerance used was of $1 \cdot 10^{-4}$ and the global tolerance was of $5 \cdot 10^{-4}$. The results presented are related to the relative vertical displacement of the crack ends. This measure

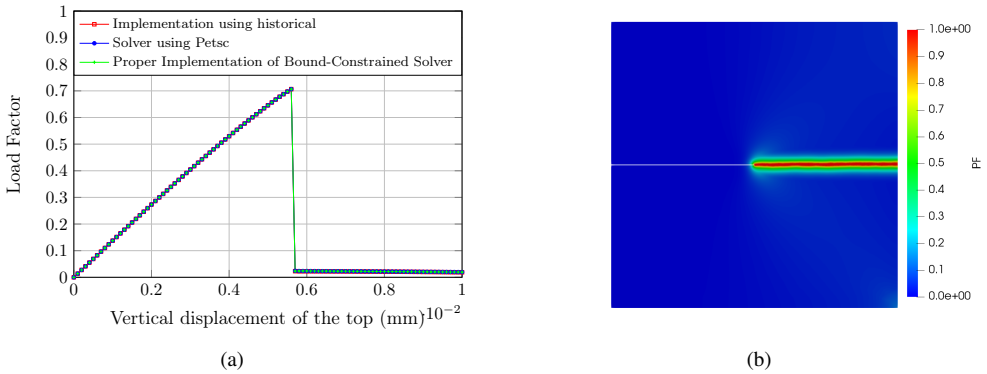

(a) (b)

Figure 4. (a) Load-displacement curves of the top edge for tension test for each solver (b) Phase-field contour plots for Tension Test

.

is known as CMSD ("Crack Mouth Sliding Displacement").

For this numerical model, four combinations of values of f_t and G_c were considered. These four combinations refer to the range of values obtained by M. Arrea [11], that is, combination of the maximum and minimum values obtained f_t and G_c in the experimental results. Case one is $f_t = 2.8\text{MPa}$ and $Gc = 0.10\text{N/mm}$, case two is $f_t = 2.8\text{MPa}$ and $Gc = 0.14\text{N/mm}$, case three is $f_t = 4.0\text{MPa}$ and $Gc = 0.10\text{N/mm}$, case four is $f_t = 4.0\text{MPa}$ and $Gc = 0.14\text{N/mm}$. The results are in Fig. 6.

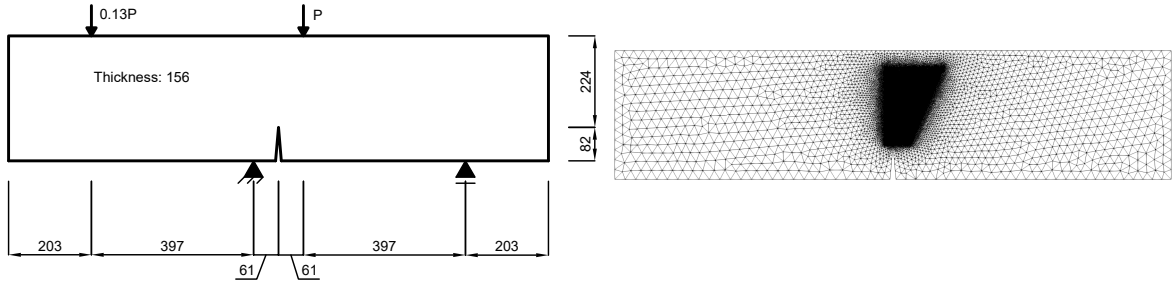

(a) (b)

Figure 5. Single-edge notched beam test. (a) Problem setting.(b) T3 mesh ($h = 25$ mm in the unrefined region and $h = 1.25$ mm in the refined region)

Comparing case 1 with case 2, it can be seen that increasing G_c slightly increases the maximum peak load of the curve. It also increases the strength of the material as the area under the curve has increased. Now comparing case 1 with case 3, it can be seen that increasing f_t increases the maximum peak load much more, but the material has more brittle behavior, as there is a faster decrease in the load in relation to the displacement in the case 3. The results for phase-field modeling do not fully match the experimental results, but the shapes of the responses are similar. The results may improve with other values of l_0, c_1, c_2 and c_3, thus calibrating the material better.

5 Conclusions

It can be concluded that the bound-constrained solver through binding with PETSc was successfully implemented, enabling to explore differents crack geometry functions and different energy degradation functions, without limitations. With example single-edge notched beam test, showed that the adopted phase-field model does not have a good result, but it presents similar shapes of response. Therefore, depending on the problem, a precaution must be taken with the phase-field model being to be used. Furthermore, with this model one can see expected effects with the modification of the f_t and G_c parameters.

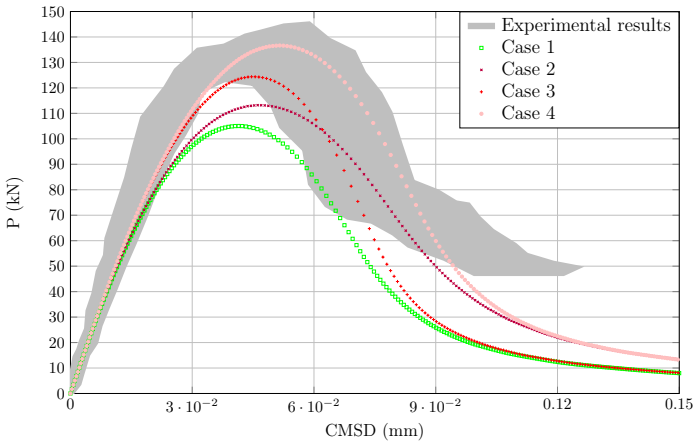

Figure 6. Response Load x CMSD, where experimental results are from M. Arrea [11]

Acknowledgements. The authors gratefully acknowledge the important support of the following Brazilian agencies FAPEMIG (in Portuguese "Fundação Nacional de Amparo à Pesquisa de Minas Gerais" - Grant PPM-00747-18), CNPq (in Portuguese "Conselho Nacional de Desenvolvimento Científico e Tecnológico" - Grants 309515/2017-3) and CAPES (in Portuguese "Coordenação de Aperfeiçoamento de Pessoal de Nível Superior").

Authorship statement. The authors hereby confirm that they are the sole liable persons responsible for the authorship of this work, and that all material that has been herein included as part of the present paper is either the property (and authorship) of the authors, or has the permission of the owners to be included here.

References

[1] J. Y. Wu, V. P. Nguyen, C. T. Nguyen, D. Sutula, S. Sinaie, and S. Bordas. Phase-field modelling of fracture. *Advances in Applied Meechanics*, vol. 53, pp. 1–183, 2020.
[2] S. Balay, S. Abhyankar, M. F. Adams, J. Brown, P. Brune, K. Buschelman, L. Dalcin, A. Dener, V. Eijkhout, W. D. Gropp, D. Karpeyev, D. Kaushik, M. G. Knepley, D. A. May, L. C. McInnes, R. T. Mills, T. Munson, K. Rupp, P. Sanan, B. F. Smith, S. Zampini, H. Zhang, and H. Zhang. PETSc users manual. Technical Report ANL-95/11 - Revision 3.14, Argonne National Laboratory, 2020.
[3] J.-Y. Wu. A unified phase-field theory for the mechanics of damage and quasi-brittle failure. *Journal of the Mechanics and Physics of Solids*, vol. 103, pp. 72–99, 2017.
[4] B. Bourdin, G. Francfort, and J. J. Marigo. Numerical experiments in revisited brittle fracture. *Journal of the Mechanics and Physics of Solids*, vol. 48, pp. 797–826, 2000.
[5] C. Miehe, F. Welschinger, and M. Hofacker. Thermodynamically consistent phase-field models of fracture: Variational principles and multi-field fe implementations. *International Journal for Numerical Methods in Engineering*, vol. 83, pp. 1273–1311, 2010.
[6] H. M. Leão. A critical study on phase-field modeling of fracture. Master's thesis, UFMG - Unversidade Federal de Minas Gerais, Belo Horizonte, MG, Brasil, 2021.
[7] P. Farell and C. Maurini. Linear and nonlinear solvers for variational phase-field models of brittle fracture. *International Jounal for Numerical Methods in Engineering*, vol. 109, pp. 648–667, 2017.
[8] J. Wu. Robust numerical implementation of non-standard phase-field damage models for failure in solids. *Computer methods in applied mechanics and engineering*, vol. 340, pp. 767–797, 2018.
[9] S. Benson and T. Munson. Flexible complementarity solvers for large-scale applications. *Optimization Methods and Software*, vol. 21, pp. 155–168, 2006.
[10] G. M. Azevedo. Implementação paralela para análises estáticas lineares pelo métodos dos elementos finitos. Master's thesis, UFMG - Federal Universit of Minas Gerais, Belo Horizonte, MG, Brasil, 2019.
[11] A. I. M. Arrea. Mixed-mode crack propagation in mortar and concrete. Technical Report No. 81-13, Department of Structural Engineering, Cornell University, Ithaca, NY, 1982.